Atomic structure of (111) twist grain boundaries in f.c.c. metals

De Hosson, J.T.M.; Vitek, V.

Atomic structure of (111) twist grain boundaries in f.c.c. metals

By J. Th. M. De Hosson and V. Vitek†

Department of Applied Physics, Materials Science Centre, University of Groningen,
Nijenborgh 18, 9747 AG Groningen, The Netherlands

ABSTRACT

In this paper we have studied the atomic structures of (111) twist boundaries and investigated the applicability of the structural unit model which has previously been established for tilt boundaries and (001) twist boundaries by Sutton and Vitek. The calculations were carried out using two different descriptions of interatomic forces. A pair potential for aluminium, for which the calculations were made at constant volume, and a many-body potential for gold, for which the calculations were performed at constant pressure. The atomic structures of all the boundaries studied were found to be very similar for both the descriptions of atomic interactions. This suggests that the principal features of the structure of (111) twist boundaries found in this study are common to all f.c.c. metals. At the same time it supports the conclusion that calculations employing pair potentials are fully capable of revealing the generic features of the structure of grain boundaries in metals. The results obtained here, indeed, show that structures of all the boundaries with misorientations between 0° and 21·79° ($\Sigma = 21$) are composed of units of the ideal lattice and/or the $\frac{1}{6}\langle 112 \rangle$ stacking fault on (111) planes, and units of the $\Sigma = 21$ boundary. Similarly, structures of boundaries with misorientations between 21·79° and 27·8° ($\Sigma = 13$), 27·8° and 38·21° ($\Sigma = 7$) and 38·21° and 60° ($\Sigma = 3$) can all be regarded as decomposed into units of the corresponding delimiting boundaries. Therefore we conclude that the atomic structure of (111) twist boundaries can well be understood in the framework of the structural unit model. A related aspect analysed here in detail is the dislocation content of these boundaries. This study shows both the general relation between dislocation content and atomic structure of the boundaries, which is an integral part of the structural unit model, and features specific to the dislocation networks present in the (111) twist boundaries. Furthermore, the dislocation content revealed by the atomistic calculations can be compared in several cases with transmission electron microscope (TEM) observations and the results are discussed in this context.

§ 1. INTRODUCTION

Grain boundary phenomena usually take place in a very narrow region, of the order of a few atomic spacings, where the two grains meet. Hence understanding of the atomic structure of grain boundaries is a necessary precursor for the development of microscopic theories of boundary properties. For this reason the structure of grain boundaries has been investigated extensively in the last decade, both experimentally and with the help of computer simulations (see the proceedings of conferences edited by

---

† Permanent address: Department of Materials Science & Engineering, University of Pennsylvania, Philadelphia 19104, U.S.A.

Rühle, Balluffi, Fischmeister and Sass (1985), Ishida (1986), Sass and Raj (1988) and Yoo, Briant and Clark (1988)). Such calculations contributed very significantly to our understanding of general features of grain boundary structure even though they were usually made using pair-potentials. While this is a crude approximation for most materials, significant results of these studies have often been found to be very little dependent on interatomic forces used and are common either to whole classes of materials or certain types of grain boundaries (for reviews see Balluffi (1982), Sutton (1984), Vitek and De Hosson (1986), Balluffi, Rühle and Sutton (1987) and De Hosson and Vitek (1987)).

One general result of this type is the structural unit model which relates structures of boundaries corresponding to different misorientations of the grains. The model was originally developed for periodic tilt boundaries (Sutton and Vitek 1983). It was later extended to (001) twist boundaries (Sutton 1982, Schwartz, Sutton and Vitek 1985, Schwartz, Bristowe and Vitek 1988) and recently it was generalized to non-periodic irrational tilt grain boundaries (Sutton 1988). In the case of (001) twist boundaries structures of all boundaries in a certain misorientation range are composed of mixtures of three different structural elements. They are the units of two short-period boundaries delimiting the misorientation range and certain 'filler' units. Structures of delimiting boundaries are contiguously composed of units of one type. Structure of a boundary with the misorientation in between two neighbouring delimiting boundaries can then be regarded as one of these delimiting boundaries with a superimposed rectangular network of screw displacement-shift-complete (DSC) dislocations related to the coincidence site lattice (CSL) of this delimiting boundary. The structure of the regions in between the dislocations is composed of units of this delimiting boundary while units of the other delimiting boundary are placed at the intersections of the dislocations. The rest of the cores of the DSC dislocations is composed of the filler units. The delimiting boundaries on the basis of which the whole misorientation range of (001) twist boundaries can be described correspond to $\Sigma = 1$ (ideal crystal), $\Sigma = 13$, 17 and 5 (Schwartz et al. 1985, Vitek 1988). These boundaries can be regarded as favoured boundaries according to the definition of Sutton and Vitek (1983). However, (001) twist boundaries are a rather special case. The purpose of the present paper is, therefore, to investigate the atomic structure of another class of twist boundaries with the aim of studying which structural features are common and which are specific to twist boundaries with different boundary planes. We concentrate here on the applicability of the structural unit model and demonstrate that the atomic structures of (111) twist boundaries can be well understood in this framework. A related aspect analysed here in detail is the dislocation content of these boundaries. This study shows both the general relation between dislocation content and atomic structure of the boundaries, which is an integral part of the structural unit model, and features specific to the dislocation networks present in the (111) twist boundaries. Furthermore, the dislocation content revealed by the atomistic calculations can be compared in several cases with transmission electron miscroscope (TEM) observations (Scott and Goodhew 1981, Hamelink and Schapink 1981, De Hosson, Schapink, Heringa and Hamelink 1986, Forwood and Clarebrough 1985, 1986) and the results are discussed in this context.

§ 2. GENERAL FEATURES OF THE DISLOCATION CONTENT OF (111) TWIST BOUNDARIES

The most important symmetry element governing structural features of (111) twist boundaries is the [111] threefold screw axis of the cubic lattice, which any dislocation

network present in these boundaries must possess. The results of atomistic studies, described in the following sections, show that such networks are either triangular or hexagonal. In general, such a network consists of three different types of dislocations with Burgers vectors $\mathbf{b}_i$ ($i = 1, 2, 3$) for which

$$\sum_i \mathbf{b}_i = 0. \tag{1}$$

The average separation, d, of dislocations in each set, is determined by Frank's formula (Frank 1950). Following Hirth and Lothe (1982), this condition can be expressed most conveniently by introducing the vectors

$$\mathbf{N}_i = N_i (\mathbf{n} \times \boldsymbol{\xi}_i), \tag{2}$$

where $\mathbf{n}$ is the unit vector in the direction of the boundary normal and $\boldsymbol{\xi}_i$ is the unit vector in the direction of the dislocations of type i.

$$N_i = 2d_i \sin\left(\frac{\Delta\Theta}{2}\right)^{-1} \tag{3}$$

where $\Delta\Theta$ is the misorientation across the boundary away from a reference state and d_i the average separation of dislocations of the set i. Owing to the threefold symmetry

$$\sum_i \mathbf{N}_i = 0, \tag{4}$$

and the magnitudes of all three vectors $\mathbf{N}_i$ are the same. Hence all the average separations d_i are also the same and in the following they are marked d. Noting that the rotation axis is in this case parallel to the boundary normal, Frank's formula reads

$$\mathbf{V} \times \mathbf{n} = \sum_i \mathbf{b}_i (\mathbf{N}_i \cdot \mathbf{V}), \tag{5}$$

where $\mathbf{V}$ is an arbitrary vector in the boundary plane.

Using conditions (1) and (4), eqn. (5) can be written as

$$\mathbf{V} \times \mathbf{n} = (2\mathbf{b}_1 + \mathbf{b}_2)(\mathbf{N}_1 \cdot \mathbf{V}) + (2\mathbf{b}_2 + \mathbf{b}_1)(\mathbf{N}_2 \cdot \mathbf{V}), \tag{6}$$

and since it has to be satisfied for any vector $\mathbf{V}$ it represents six linear equations for the components of the vectors $\mathbf{N}_1$ and $\mathbf{N}_2$. In the coordinate system for which the x axis is parallel to the boundary normal, $\mathbf{n}$, and the y axis is parallel to the projection of the Burgers vector $\mathbf{b}_1$ in the boundary plane, the solution is $\mathbf{N}_1 = (1/b)[0, -2/3, 0]$ and $\mathbf{N}_2 = (1/b)[0, -1/3, 1/\sqrt{3}]$, where b is the magnitude of the projection of the Burgers vectors of the dislocations to the boundary plane; owing to the threefold symmetry b is the same for all three types of dislocations. The Burgers vectors of these dislocations may have components perpendicular to the boundary but it follows from eqns. (1) and (6) that these components have to satisfy the conditions $b_2 \perp = b_3 \perp = -b_1 \perp / 2$. However, all the dislocations found in the present atomistic studies have Burgers vectors parallel to the boundary plane.

When the vectors $\mathbf{N}_1$ and $\mathbf{N}_2$ are known the average separation of the dislocations of the network can be found using eqn. (3). In the present case this gives

$$d = \frac{3b}{4 \sin\left(\frac{1}{2}\Delta\Theta\right)}. \tag{7}$$

In the case of regular triangular networks this is directly the separation of the dislocations forming the sides of the triangles. In regular hexagonal networks dislocations forming a given set of parallel sides of the hexagons are effectively broken into segments the total length of which is equal to the one third of the length these dislocations would have if they were not segmented. Hence the separation of the dislocations forming a given set of the sides of the hexagons is equal to $d/3$.

When well localized dislocations can be identified in grain boundaries a significant elastic energy is associated with such a network. This was first recognized by Read and Shockley (1950), who evaluated this energy as a function of $\Delta\Theta$ for pure tilt boundaries and showed that it is responsible for the existence of cusps on a plot of the energy against misorientation dependence for misorientations corresponding to certain special boundaries which serve as reference structures for other grain boundaries. An exact evaluation of the elastic energy of a tilt boundary as the strain energy of a wall of edge dislocations is presented in Hirth and Lothe (1982) for the case of isotropic elasticity. Using the same method, the elastic energy of a rectangular network of screw dislocations, applicable to (001) twist boundaries, has recently been derived by Vitek (1987), and we present here a similar calculation for the network composed of three sets of screw dislocations, which is a good approximation for dislocation networks found in (111) twist boundaries.

To evaluate the elastic energy of a network of screw dislocations, we consider in a similar fashion to Hirth and Lothe (1982, p. 740), a pair of such networks of opposite sign formed in an infinite crystal. The specific energy of formation of such a pair, when well separated, is then twice the energy per unit area of the network. The average separation of the dislocations in this network given by Frank's formula, eqn. (7), is d, and owing to the threefold symmetry the average length of the dislocations separated by d is $l=2d/\sqrt{3}$. Let us take the plane of the boundary as the zy plane with one set of dislocations parallel to the z axis. The force in the direction x (perpendicular to the boundary) per unit length of a dislocation of opposite sign which lies parallel to the z axis is $-\sigma_{23}b$, where b is the magnitude of its Burgers vector and σ_{23} the corresponding component of the stress field associated with the network in the zy plane. The energy per length l per dislocation in one boundary can then be calculated as one half of the interaction energy of this dislocation with the dislocation network and is equal to

$$W=\frac{1}{2}\int_0^l\int_{r_0}^\infty \sigma_{23}\,b\,dx\,dz,\tag{8}$$

where r_0 is the core radius of the dislocations. The elastic energy per unit area of the boundary is then

$$\gamma_{el}=\frac{W}{S}=\frac{3\sqrt{3}}{2}\frac{W}{d^2},\tag{9}$$

where $S=l^2/2\sqrt{3}=2d^2/3\sqrt{3}$ is the area per dislocation segment of length l.

In the framework of the linear isotropic elasticity the stress field associated with the dislocation network can be evaluated as a sum of the stresses of individual dislocations. Following the same procedure as employed in the case of the wall of edge dislocations

by Hirth and Lothe (1982, p. 731), we obtain for the network of three screw dislocations related by a threefold axis symmetry operation

$$
\sigma_{23} = \frac{Gb}{2d} \left[\frac{2\sinh\left(\dfrac{2\pi x}{d}\right)}{\cosh\left(\dfrac{2\pi x}{d}\right) - \cos\left(\dfrac{2\pi y}{d}\right)} - \frac{\sinh\left(\dfrac{2\pi x}{d}\right)}{\cosh\left(\dfrac{2\pi x}{d}\right) - \cos\left(\dfrac{\pi(z\sqrt{3}+y)}{d}\right)} \right.
$$

$$
\left. - \frac{\sinh\left(\dfrac{2\pi x}{d}\right)}{\cosh\left(\dfrac{2\pi x}{d}\right) - \cos\left(\dfrac{\pi(z\sqrt{3}-y)}{d}\right)} \right], \tag{10}
$$

where G is the shear modulus. After inserting eqn. (10) into eqns. (8) and (9) (for $y=0$) and carrying out the integration as in Vitek (1987), we obtain

$$
\gamma_{el} = \frac{Gb^2\sqrt{3}}{8\pi^2 d} \{\ln\left[\cosh\alpha + (\cosh\alpha^2 - 1)^{1/2}\right] - \ln(\cosh\alpha - 1) - \ln 2\}, \tag{11}
$$

where $\alpha = 2\pi r_0/d$. For small misorientations, when $\Delta\Theta \ll 1$, $d \approx 3b/2\,\Delta\Theta \gg r_0$ and $\alpha \ll 1$, we can write $\cosh\alpha \approx 1 + \alpha^2/2$. Equation (11) then gives, when neglecting in the curly brackets all the terms of order higher than α,

$$
\gamma_{el} = \frac{Gb^2\sqrt{3}}{4\pi d} \left[\frac{\pi r_0}{d} - \ln\left(\frac{2\pi r_0}{d}\right)\right]. \tag{12}
$$

Using the above expression for d we obtain

$$
\gamma_{el} = \frac{Gb\sqrt{3}}{6\pi} \left[\frac{2\pi r_0}{3b}\Delta\Theta + \ln\left(\frac{3b}{4\pi r_0}\right) - \ln\Delta\Theta\right]\Delta\Theta \tag{13}
$$

This formula is very similar to that obtained by Vitek (1987) for the square grid of screw dislocations. It should be noted that the term $(2\pi r_0/3b)\,\Delta\Theta$ inside the square brackets in eqn. (13) cannot be neglected with respect to other terms, in general, particularly when $b \ll r_0$; this is often the case for grain boundary dislocations whose Burgers vectors are usually smaller than the spacing of nearest neighbours, which is a lower limit for r_0. No such term exists in the same approximation when evaluating the energy of a wall of edge dislocations (Hirth and Lothe 1982, Vitek 1987).

The energy of the grain boundary is then

$$
\gamma = \gamma_0 + 2E_c/b + \gamma_{el}, \tag{14}
$$

where E_c is the core energy (per unit length) of the dislocation and γ_0 is the energy of the corresponding reference state. This leads to the energy against misorientation dependence with cusps at $\Delta\Theta = 0$ (i.e. at misorientations corresponding to the favoured boundaries, which has indeed been found in the present study).

§3. METHOD OF ATOMISTIC CALCULATIONS AND INTERATOMIC FORCES

The method of calculation was principally the same as in a number of previous studies and has been described in detail elsewhere (Vitek, Sutton, Smith and Pond 1980). A block consisting of the atomic coordinates of an unrelaxed f.c.c. bicrystal, containing the chosen coincidence boundary, is first constructed in the computer using

the basic geometrical rules of the CSL. The periodicity imposed by the CSL in the boundary plane is then maintained during the relaxation. A relaxed structure is found by minimizing the total internal energy with respect to all atomic positions *and* the relative displacements of the adjoining grains. During the relaxation, relative displacements of atomic layers parallel to the boundary are also permitted and thus the net relative translation of the two grains occurs automatically. The relaxation procedure was a standard gradient method.

Two different descriptions of atomic interactions were used in this paper. One is the pair potential for aluminium constructed by Dagens, Rasolt and Taylor (1975) on the basis of the pseudo-potential theory. It possesses long-range Friedel oscillations but it was shown that these oscillations can be damped (Duesberry, Jacucci and Taylor 1979, Pettifor and Ward 1984) and thus it is reasonable to limit the interactions to a small number of neighbours. In the present case the interaction extends up to the fourth-neighbour shell. Pair potentials are generally density-dependent and the total energy contains a large volume term which contributes the major part of the total energy. Nevertheless, structural features of those defects which do not involve large density and coordination variation, like grain boundaries in metals, can be successfully investigated with the use of pair potentials, but the calculations have to be carried out at constant volume. In the present study this has been ensured by not allowing any total displacement of the grains perpendicular to the boundary plane. However, the complete evaluation of the energy requires inclusion of the density-dependent term and for this reason we do not report here the boundary energies for aluminium.

The other description of interactions used in the present calculations was the many-body potential for gold constructed recently by Ackland, Tichy, Vitek and Finnis (1987) using the general concept introduced by Finnis and Sinclair (1984). In this framework the total energy of a system of N atoms is written as

$$E_{tot} = \frac{1}{2} \sum_{i,j=1}^{N} V(r_{ij}) - \sum_{i} \left(\sum_{j} \phi(r_{ij}) \right)^{1/2}, \qquad (15)$$

where both V and ϕ are pair potentials fitted empirically to reproduce the equilibrium lattice parameter, elastic constants, cohesive energy and vacancy formation energy. The first term in eqn. (15) is the pair interaction which is repulsive at small separation of atoms while the second term is always attractive and replaces the above mentioned density-dependent term accompanying the pair potentials.

When using the many-body potentials the calculation can be done at constant pressure and the energy always fully evaluated. Hence all the calculations employing the many-body potential for gold were carried out at constant pressure, which means that an overall expansion was allowed, and the energies of the corresponding boundaries are reported. However, in all cases studied, the atomic structures found when using the pair potential for aluminium and the many-body potentials are very similar and for this reason we only show structures obtained in the pair-potential studies. For a more detailed discussion of the effect of interatomic potential on computed structures reference is made to Vitek and De Hosson (1986) and Wolf and Lutsko (1989).

§4. ATOMIC STRUCTURE OF GRAIN BOUNDARIES

Owing to the threefold symmetry of the [111] axis and the twofold symmetry of the [110] axis which lies in the (111) plane, the misorientations for which different

Misorientations and energies of (111) twist boundaries (calculated using a many-body potential for gold).

Θ	Σ	$E(\text{mJ m}^{-2})$
7·34	183	190·0
11·63	73	224·0
13·17	57	228·0
15·18	43	233·0
17·89	31	240·0
21·79	21	237·0
24·43	67	245·5
26·01	237	247·0
27·80	13	246·0
29·41	291	248·0
30·59	97	251·0
32·31	39	248·0
33·99	79	246·0
35·57	201	243·0
38·21	7	238·0
43·57	49	236·0
46·83	19	224·5
50·57	37	210·0
52·66	61	191·5
53·99	91	189·2
60·00	3	17·3

Fig. 1
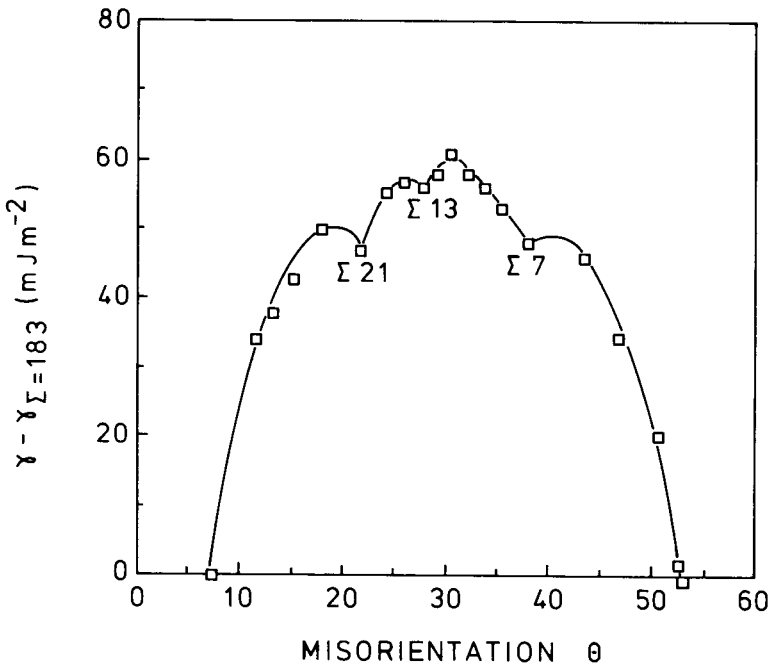
Energy against misorientation calculated using the many-body potential for gold. The squares represent values found in the atomistic calculations while the solid curve is an interpolation obtained when assuming the dependence of the type given by eqn. (14).

boundaries are found can be limited to the range 0° and 60°. In fact, it is the symmetry of the corresponding delimiting CSL boundaries ($\Sigma = 21, 13, 7$ and 3) which has to be taken into account, instead of the lattice symmetry. The corresponding CSLs have a third-order symmetry as well as a second-order one implied by the CSL 180° rotation axis (Bleris and Delavignette 1981, Doni, Bleris, Karakostas, Antonopoulos, Delavignette 1985). In this misorientation range we have simulated 21 different coincidence boundaries. Their reciprocal coincidence site densities, Σ, misorientation Θ, and energies found when using the many-body potential for gold, are summarized in the table. The dependence of grain boundary energy on misorientation is shown in fig. 1. Cusps are clearly visible at misorientations corresponding to $\Sigma = 21, 13, 7$ and 3, suggesting a special nature of these boundaries. The analysis of structures of these boundaries, presented below, indeed shows that for $0° < \Theta < 21\cdot79°$ they can be interpreted as composed of units of $\Sigma = 1$ and $\Sigma = 21$ boundaries; in the former case, units of the ideal crystal or the $\frac{1}{6}\langle 112\rangle(111)$ stacking fault occur in the boundary. For $21\cdot79° < \Theta < 27\cdot80°$ the boundary structures are composed of units of $\Sigma = 21$ and $\Sigma = 13$ boundaries, for $27\cdot80° < \Theta < 38\cdot21°$ of units of $\Sigma = 13$ and $\Sigma = 7$ boundaries, and for $38\cdot21° < \Theta < 60°$ of units of $\Sigma = 7$ and $\Sigma = 3$ boundaries. Hence, the short period boundaries corresponding to $\Sigma = 21, 13, 7$ and 3 are the favoured boundaries as defined by Sutton and Vitek (1983) and we first present their atomic structure and summarize possible related grain boundary dislocations.

4.1. Structure of favoured boundaries

The atomic structure of the $\Sigma = 21$ boundary is shown in fig. 2. In this and all the following figures the symbols $\triangle$, $+$, $\square$, $*$ represent atoms in four different (111) planes adjacent to the boundary; the boundary plane is located between layers marked $+$ and $\square$. The fundamental structural unit of this boundary has the form of a hexagon and is delineated in fig. 2 by solid lines. The shortest DSC vectors related to this coincidence are of the type $(1/42)[\bar{5}41]$ and dislocations with this Burgers vector are associated with a step of height equal to the interplanar spacing of (111) planes (King 1982). On the other hand no steps are associated with the DSC dislocations having the Burgers vectors $(1/14)[\bar{3}21]$ or $(1/14)[\bar{5}41]$. All these dislocations have been identified in boundaries in the misorientation range $0° < \Theta < 21\cdot79°$.

The atomic structure of the $\Sigma = 13$ boundary is shown in fig. 3, where the basic structural unit is again delineated by solid lines. The shortest DSC vector corresponding to this coincidence is $(1/26)[\bar{4}31]$ and no steps are associated with these dislocations. Two possible atomic structures of the $\Sigma = 7$ boundary were found which differ in the relative displacement of the adjoining grains by $(1/28)[\bar{3}21]$; they are shown in figs. 4 (a) and (b) respectively. The shortest DSC vectors ascribed to this coincidence are of the type $(1/14)[\bar{3}21]$ and no steps are associated with these dislocations. The structure shown in fig. 4 (a) possesses a somewhat lower energy and is found in boundaries containing units of the $\Sigma = 7$ boundary.

The $\Sigma = 3$ boundary, which is the usual twin boundary in f.c.c. crystals, is also a favoured boundary. It is not shown here for reason of space, since its structure is commonly known, but units of this boundary are seen in fig. 11. The shortest DSC vector corresponding to this coincidence is $\frac{1}{6}[\bar{2}11]$. Dislocations with this Burgers vector are associated with a step of height one interplanar spacing of (111) planes.

Fig. 2
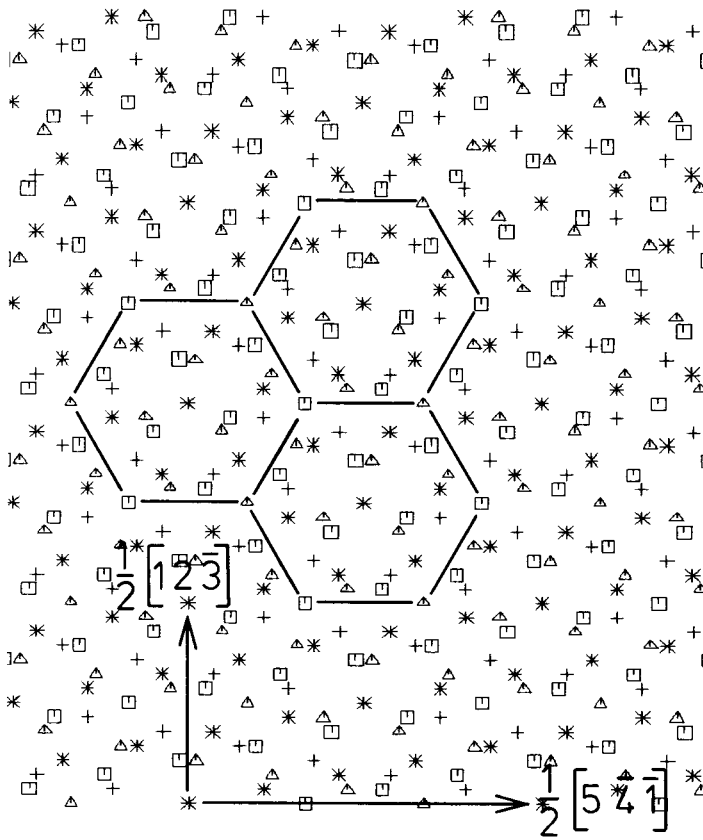
Structure of the $\Sigma = 21$ boundary.

4.2. *Low-angle boundaries $0° < \Theta < 21.78°$*

A typical example of a low-angle grain boundary is that for $\Sigma = 183(\Theta = 7.34°)$. Its decomposition into the structural units which corresponds to decomposing the shortest CSL vector according to

$$\tfrac{1}{2}[5\bar{9}4] \rightarrow \tfrac{1}{2}[2\bar{3}1] + 9\tfrac{1}{6}[1\bar{2}1] \tag{15}$$

is depicted in fig. 5. The hexagons are clearly the units of the $\Sigma = 21$ boundary. The regions connecting $\Sigma = 21$ units correspond to the cores of grain boundary dislocations which intersect at the minority $\Sigma = 21$ units, in a similar manner to the case of (001) twist boundaries (Schwartz *et al.* 1985). As shown below, these dislocations appear to be the three partial dislocations of the type $\tfrac{1}{6}\langle 112 \rangle$ lying in screw orientations. The triangular regions between these dislocations are then, alternatively, the ideal crystal and the stacking fault. The Burgers vectors of the three intersecting partials are: $\mathbf{b}_1 = \tfrac{1}{6}[11\bar{2}]$, $\mathbf{b}_2 = \tfrac{1}{6}[1\bar{2}1]$ and $\mathbf{b}_3 = \tfrac{1}{6}[\bar{2}11]$. Taking the ideal crystal as the reference structure, the average separation of the dislocations of the same type in the network is, according to Frank's formula (eqn. (7)), $d = 4.782a_0$, where a_0 is the lattice parameter. It is seen from
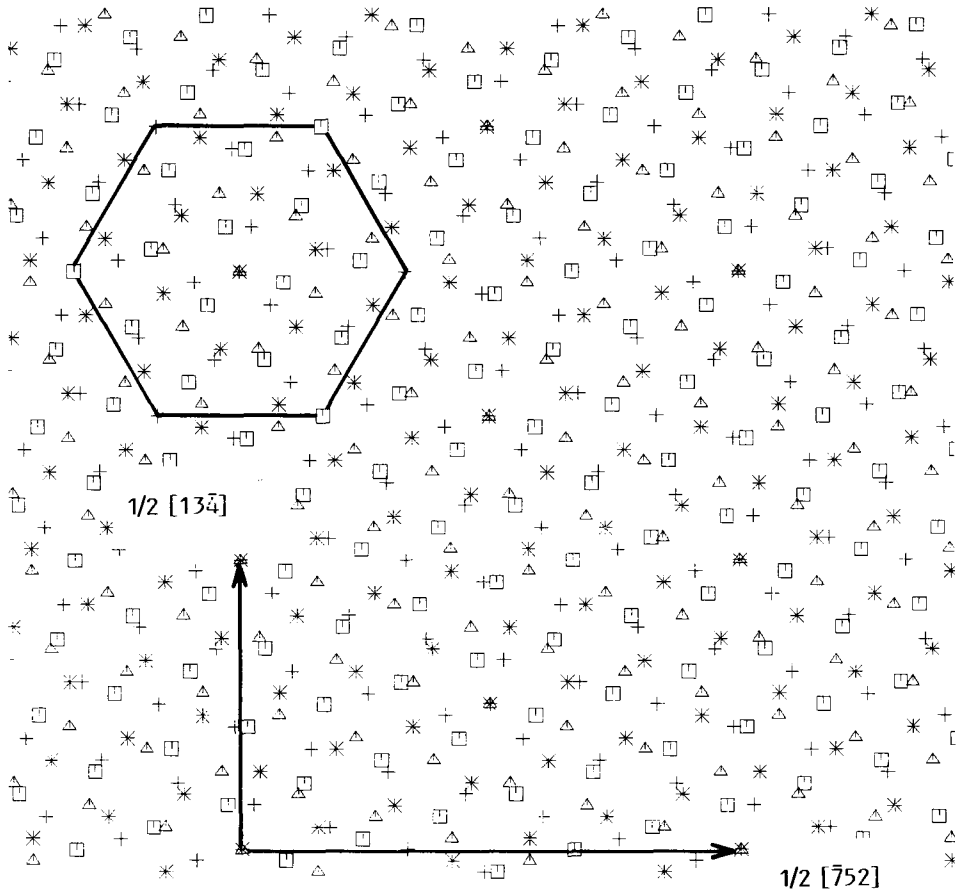
Fig. 3

Structure of the $\Sigma = 13$ boundary.

fig. 5 that the separation of the dislocations is $|\frac{1}{4}[14\,\overline{13}\,\overline{1}]| = 4 \cdot 782 a_0$, in agreement with Frank's rule.

For the $\Sigma = 57$ boundary, where the ratio of ideal crystal units and $\Sigma = 21$ units is $1:1$, the situation is very similar to the case of $\Sigma = 183$ when considering the ideal crystal (together with the stacking fault) as a reference structure. The separation of the $\frac{1}{6}\langle 112 \rangle$ dislocations is now $|\frac{1}{4}[\overline{8}71]| = 2 \cdot 669 a_0$, in agreement with Frank's formula for $\Delta \Theta = 13 \cdot 7°$. However, at this point the $\Sigma = 21$ boundary can also be regarded as the reference structure and the dislocation content expressed in terms of the DSC dislocations related to this coincidence, as described below for boundaries with misorientations larger than that of $\Sigma = 57$.

When moving to angles larger than $13 \cdot 17°$, units of the $\Sigma = 21$ boundary are in the majority and the ideal crystal and/or stacking fault act as intersections of the corresponding DSC dislocations preserving the $\Sigma = 21$ structure. An example is the $\Sigma = 43$ boundary shown in fig. 6 (a). The corresponding network of grain boundary dislocations, shown schematically in fig. 6 (b), is quite complex. It consists of screw
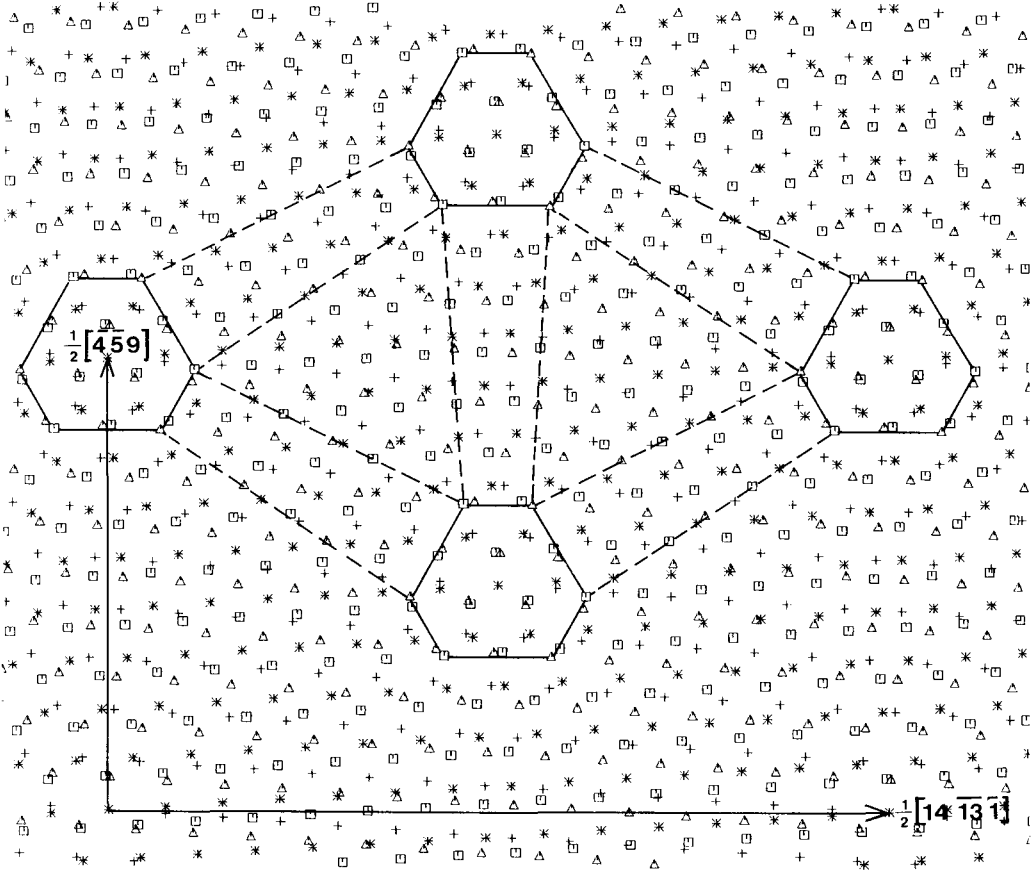
Fig. 4

$\frac{1}{2}[\bar{1}\bar{2}\,3]$

$\frac{1}{2}[5\bar{4}\,1]$

(a)

$\frac{1}{2}[12\bar{3}]$

$\frac{1}{2}[5\,\bar{4}\,1]$
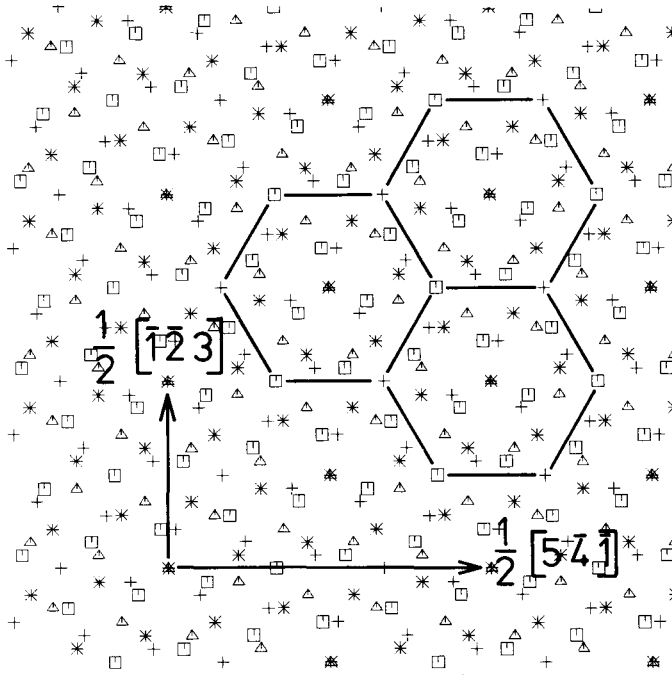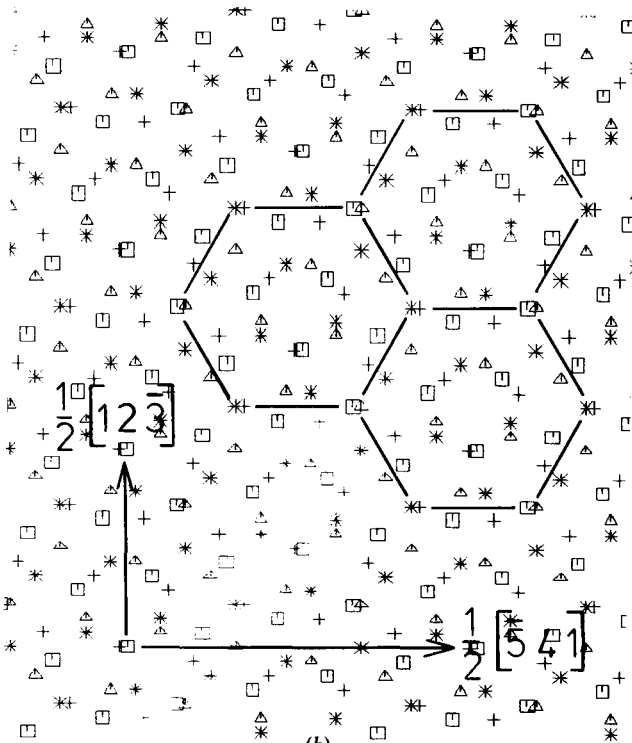
(b)

Two alternative structures of $\Sigma = 7$ which differ in the relative displacement of the adjoining grains by $(1/28)[\bar{3}21]$. The structure shown in (a) possesses a lower energy.

Fig. 5

Structure of the $\Sigma = 183$ boundary: solid lines indicate $\Sigma = 21$ units whereas the dashed lines of Shockley partial dislocations form triangular regions.

dislocations of the type $(1/14)[\bar{5}41]$ and edge dislocations of the type $(1/14)[\bar{3}21]$. These two types of dislocations are both DSC dislocations related to $\Sigma = 21$ but the latter do not contribute to the misorientation because of their edge character. The separation of the screw dislocations is found to be equal to $\frac{1}{4}|\frac{1}{2}[\overline{13}\,8\,5]| = 2\cdot008a_0$. Frank's formula based on $(1/14)[\bar{5}41]$ and $\Delta\Theta = 6\cdot609°$ with respect to $\Sigma = 21$ would predict a separation of $6\cdot023a_0$. At first sight, this seems to be in conflict but one should notice that the dislocation network is hexagonal and, as explained in §2, the separation of the dislocations is then only one third of the average separation given by Frank's formula, which is in agreement with the separation determined from fig. 6(a).
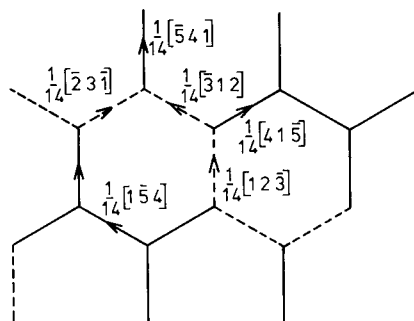
4.3. Misorientation range: $21\cdot78° < \Theta < 27\cdot80°$

The structure for $\Sigma = 67$ ($\Delta\Theta = 2\cdot646$ with respect to $\Sigma = 21$) is presented in fig. 7. The grain boundary dislocations are the DSC dislocations of the type $(1/42)[\bar{5}41]$. Their separation is $|\frac{1}{4}[\overline{16}\,11\,5]| = 5\cdot012a_0$, which is in accordance with Frank's formula
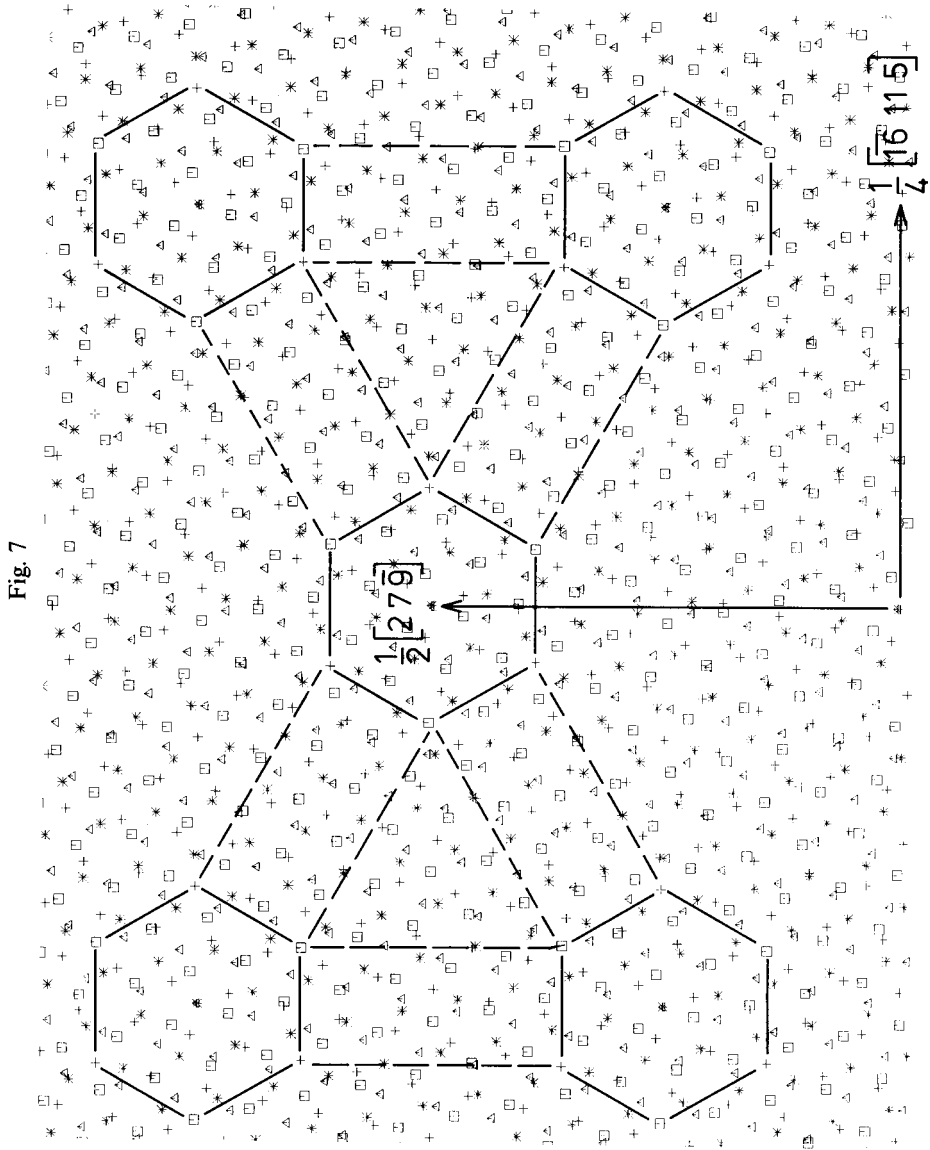
Fig. 6
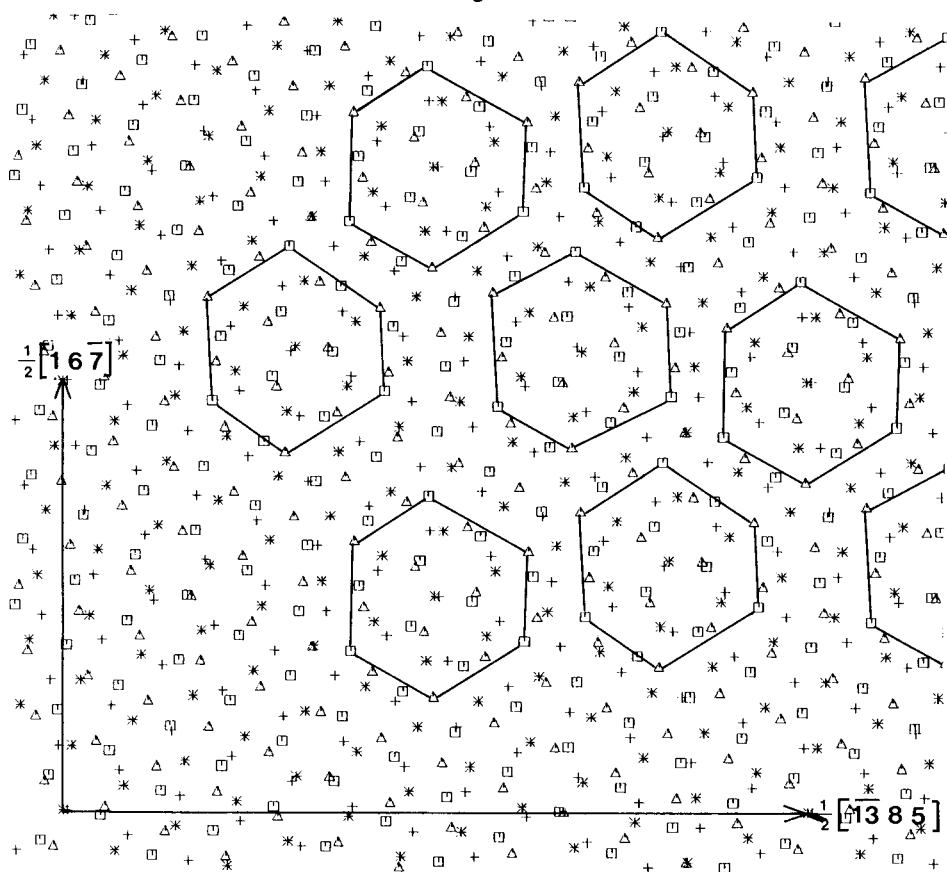
(a)

(b)

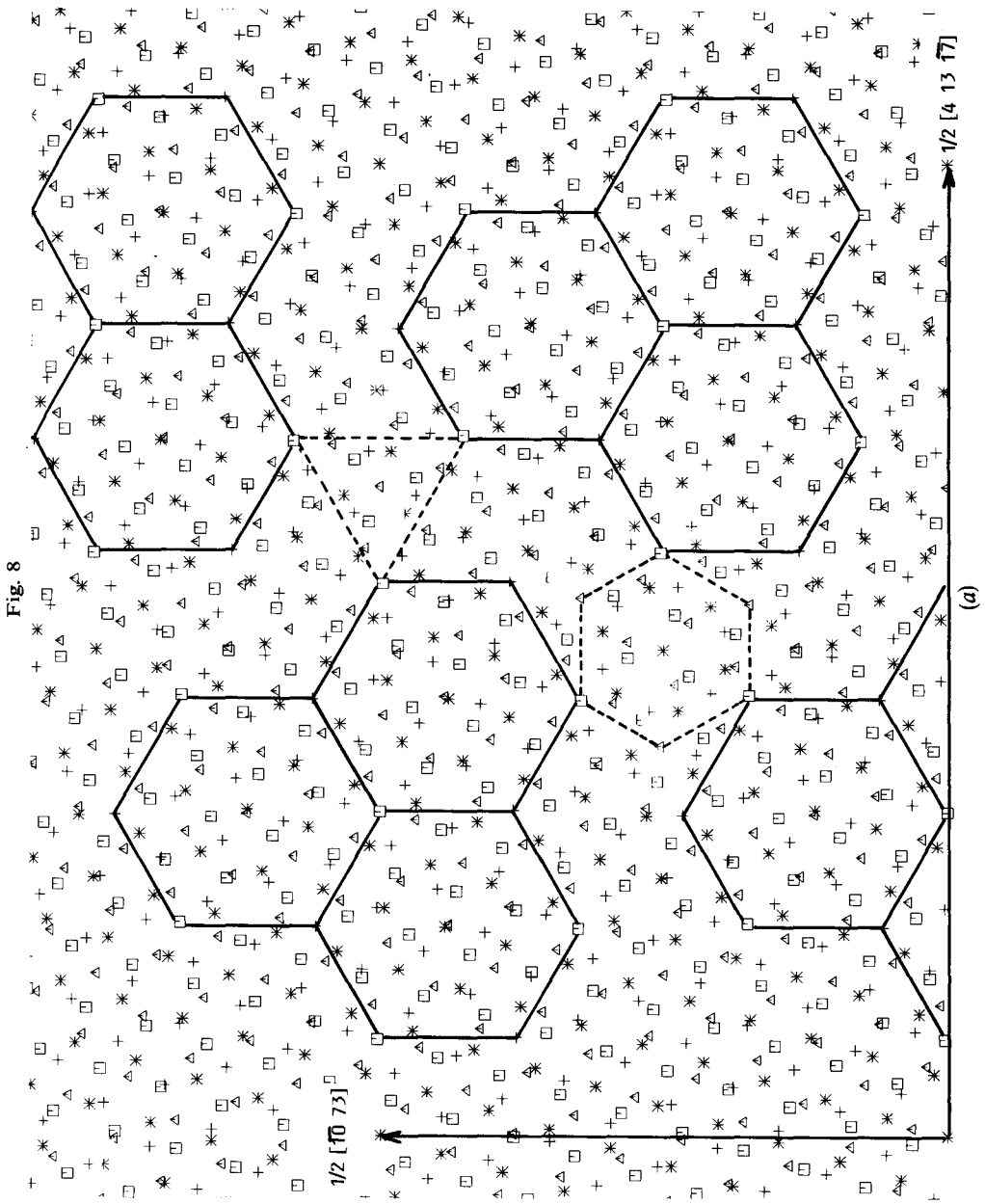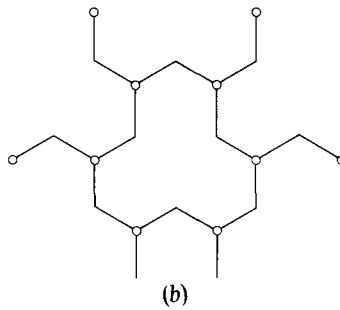(a) Structure of the $\Sigma = 43$ boundary: solid lines indicate $\Sigma = 21$ units. (b) Schematic drawing of the corresponding network of grain boundary dislocations consisting of (1/14)[$\bar{5}$41] screw and (1/14)[$\bar{3}$21] edge components.

Fig. 7

$\frac{1}{2}[2\bar{7}9]$

$\frac{1}{4}[\overline{16}\,11\,5]$

Structure of the $\Sigma = 67$ boundary. $\Sigma = 13$ units are indicated by solid lines.

Fig. 8

(b)

(a) Structure of the $\Sigma = 237$ boundary: solid lines indicate $\Sigma = 13$ units surrounded by DSC
dislocations intersecting at $\Sigma = 21$ units (dashed line). (b) Schematic drawing of grain
boundary dislocations.

(eqn. (7)). The intersections of the dislocations are now units of the $\Sigma = 13$
boundary and the dislocation network surrounds triangular areas of the $\Sigma = 21$
structures which are alternately on different levels. The reason is that the DSC
dislocations forming the network are associated with steps of height $\frac{1}{3}[111]$.

Figure 8(a) shows the structure of the $\Sigma = 237$ boundary. The regions of the
boundary, each composed of three hexagonal units of the $\Sigma = 13$ boundary, are
surrounded by DSC dislocations of the type $(1/26)[\bar{4}31]$, relating to the $\Sigma = 13$
coincidence, which form the network shown schematically in fig. 8(b). These
dislocations are not pure screw but each consists of two parts which have edge
components of opposite sign. Their intersections are units and/or parts of the units of
the $\Sigma = 21$ boundary. It is seen from fig. 8(a) that the separation of the network
dislocations with the same Burgers vector is $|\frac{1}{4}[\bar{10}\,7\,3]| = 3 \cdot 142 a_0$. According to eqn. (7)
we obtain $d = 9 \cdot 427 a_0$ for these DSC dislocations when taking the $\Sigma = 13$ boundary as
the reference structure; which means three times as much, in accordance with the fact
that the network is hexagonal.

4.4. Misorientation range $27 \cdot 8° < \Theta < 38 \cdot 21°$

The structure of the $\Sigma = 291$ boundary is shown in fig. 9. The composition of this
boundary is analogous to that for $\Sigma = 237$. The areas composed of three hexagonal
units are again regions of the slightly distorted $\Sigma = 13$ structure which are surrounded
by DSC dislocations of the type $(1/26)[\bar{4}31]$. However, the dislocations intersect at
regions corresponding to the $\Sigma = 39$ boundary. The latter can, of course, be regarded as
composed of $1:1$ mixture of units of the $\Sigma = 13$ and $\Sigma = 7$ boundaries. The structure of
the $\Sigma = 79$, shown in fig. 10, is very similar, possessing the same regions of the $\Sigma = 13$
boundary and the same dislocation network but the $(1/26)[\bar{4}31]$ dislocations intersect
at regions of the $\Sigma = 7$ boundary.

When the misorientation approaches that of the $\Sigma = 7$ boundary, the roles of $\Sigma = 7$
and $\Sigma = 13$ units interchange. For example, the structure of the $\Sigma = 201$ boundary,
which (for the reason of space) is not shown here, is analogous to that of the $\Sigma = 79$
boundary with the structural units of the $\Sigma = 13$ boundary replacing the units of the
$\Sigma = 7$ boundary and *vice versa*. The grain boundary dislocations intersecting in the
regions of the $\Sigma = 13$ boundary are now the DSC dislocations of the type $(1/14)[\bar{3}21]$,
related to the $\Sigma = 7$ coincidence.

Fig. 9

1/2 [5 14 19̄]

1/2 [1̄1̄ 83]
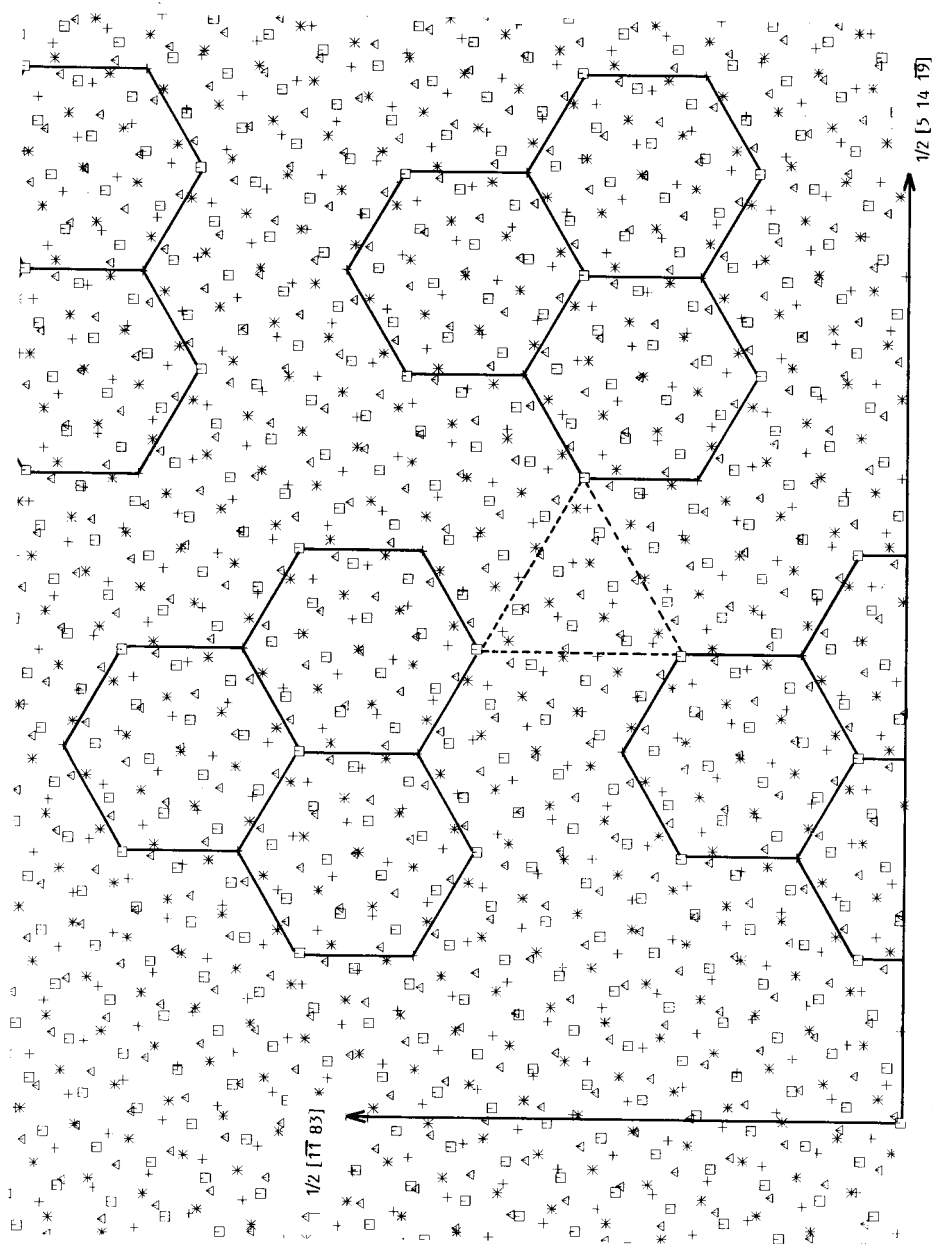
Structure of the $\Sigma = 291$ boundary: Solid lines indicate slightly distorted $\Sigma = 13$ units surrounded by dislocations intersecting at $\Sigma = 39$ units (dashed line).

Fig. 10
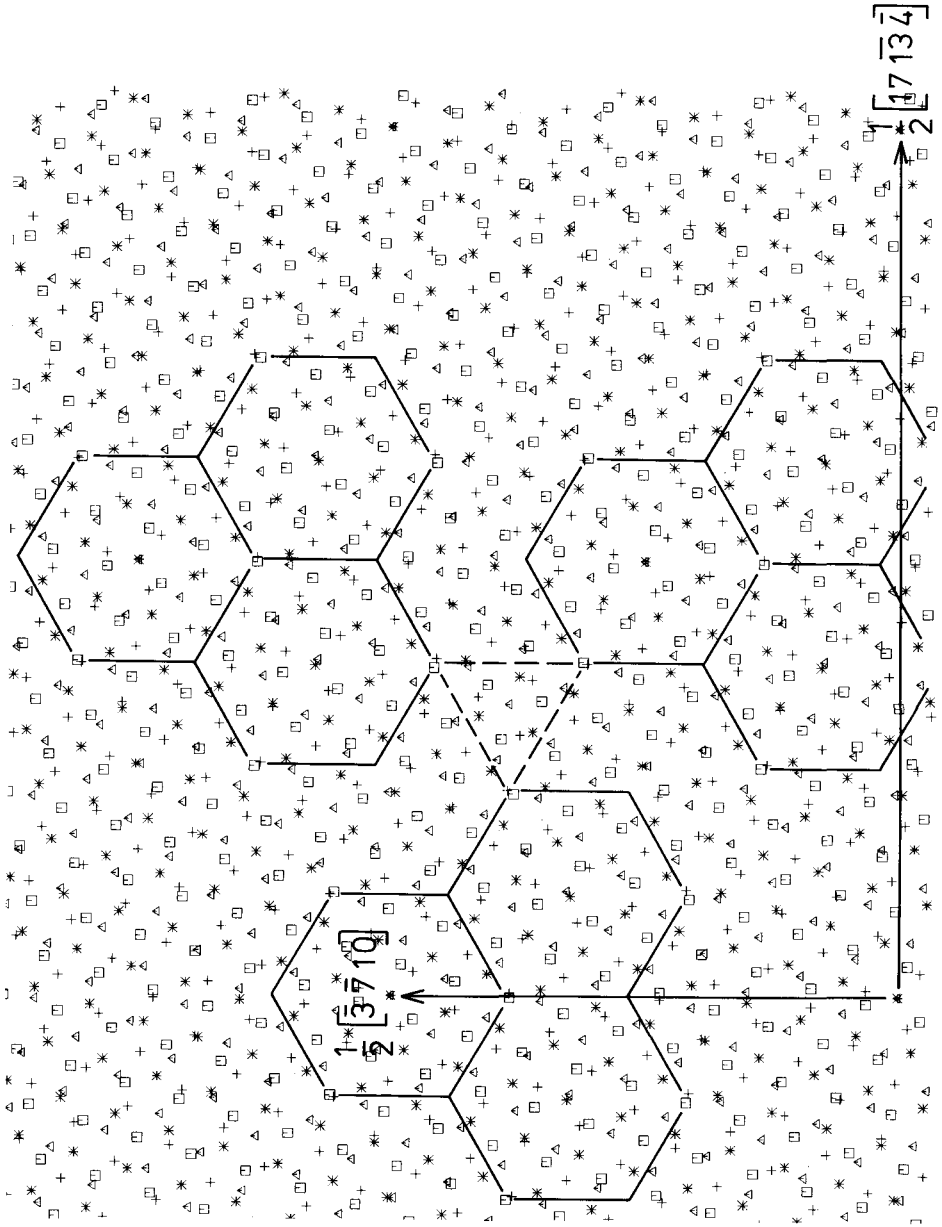
Structure of the $\Sigma = 79$ boundary: solid lines indicate $\Sigma = 13$ units surrounded by dislocations intersecting at $\Sigma = 7$ units (dashed line).

### 4.5. *Misorientation range* $38·21° < \Theta < 60°$

The structure of the $\Sigma = 49$ boundary has been found to consist of the units of the $\Sigma = 7$ structure surrounded by the network of DSC dislocations of the type $(1/14)[\bar{3}21]$ which intersect at the units of the $\Sigma = 3$ boundary. In the $\Sigma = 19$ boundary the ratio of the $\Sigma = 7$ and $\Sigma = 3$ units is $1:1$ and the structure may be described either as $\Sigma = 7$ units surrounded by the network of $(1/14)[\bar{3}21]$ dislocations intersecting at $\Sigma = 3$ units or as $\Sigma = 3$ units surrounded by the network of DSC dislocations of the type $\frac{1}{6}[\bar{2}11]$ intersecting at $\Sigma = 7$ units. For the reason of space we do not show these structures here in detail. The $\Sigma = 61$ boundary, shown in fig. 11, represents a typical boundary with the misorientation close to that of $\Sigma = 3$. The triangular regions of the $\Sigma = 3$ twin are surrounded by the network of the DSC dislocations with the Burgers vectors of the type $\frac{1}{6}[\bar{2}11]$, which intersect at highly distorted units of the $\Sigma = 7$ boundary. As seen from fig. 11, the separation of the DSC dislocations in this network is equal to $|\frac{1}{4}[\bar{14}\,13\,1]| = 4·783a_0$, which agrees with Frank's formula (eqn. (7)). The alternate regions of the $\Sigma = 3$ twins are on different levels since $\frac{1}{6}\langle 112 \rangle$ dislocations lying in the boundary are associated with steps of height $\frac{1}{3}[111]$.

§5. DISCUSSION

In this paper we have studied the atomic structures of (111) twist boundaries and investigated the applicability of the structural unit model which has previously been established for tilt boundaries and (001) twist boundaries (Sutton and Vitek 1983, Schwartz *et al.* 1985). The calculations were carried out using two differing descriptions of interatomic forces, namely a pair potential for aluminium, for which the calculations were made at constant volume, and a many-body potential for gold, for which the calculations were performed at constant pressure. The atomic structures of all the boundaries studied were found to be very similar for both descriptions of atomic interactions. This suggests that the principal features of the structure of (111) twist boundaries found in this study are common to all f.c.c. metals. At the same time it supports the conclusion, discussed in a previous paper (Vitek and De Hosson 1986), that calculations employing pair potentials are fully capable of revealing the generic features of the structure of grain boundaries in metals. In general, large differences between calculations carried out using many-body potentials and pair potentials arise only if the coordination of atoms in the core of a defect is substantially different from that in the ideal crystal, and/or when large local expansions or contractions occur. Otherwise, the many-body potentials can be well approximated by effective pair potentials, as first pointed out by Finnis and Sinclair (1984). This suggests that in twist boundaries studied here neither large expansions nor large deviations in coordination occur, as has also been confirmed by detailed inspection of the calculated structures. This is also in full agreement with the recent study of Wolf and Lutsko (1989), who carried out calculations of the structure and energy of a number of different twist boundaries using many-body potentials of the embedded atom type (Daw and Baskes 1984) and the corresponding effective pair potentials, and found no substantial differences in these two cases. Nevertheless, the use of many-body potentials is advantageous in that the calculations can be carried out straightforwardly at constant pressure, and when evaluating the energy the uncertainties arising in the case of pair potentials due to the density-dependent term are alleviated.

The structural unit model, which establishes a relationship between structures of grain boundaries with different misorientations and relates the atomic structures and

Fig. 11

$$\frac{1}{2}\left[14\bar{1}3\bar{1}\right]$$

$$\frac{1}{2}\left[\bar{4}5\bar{9}\right]$$
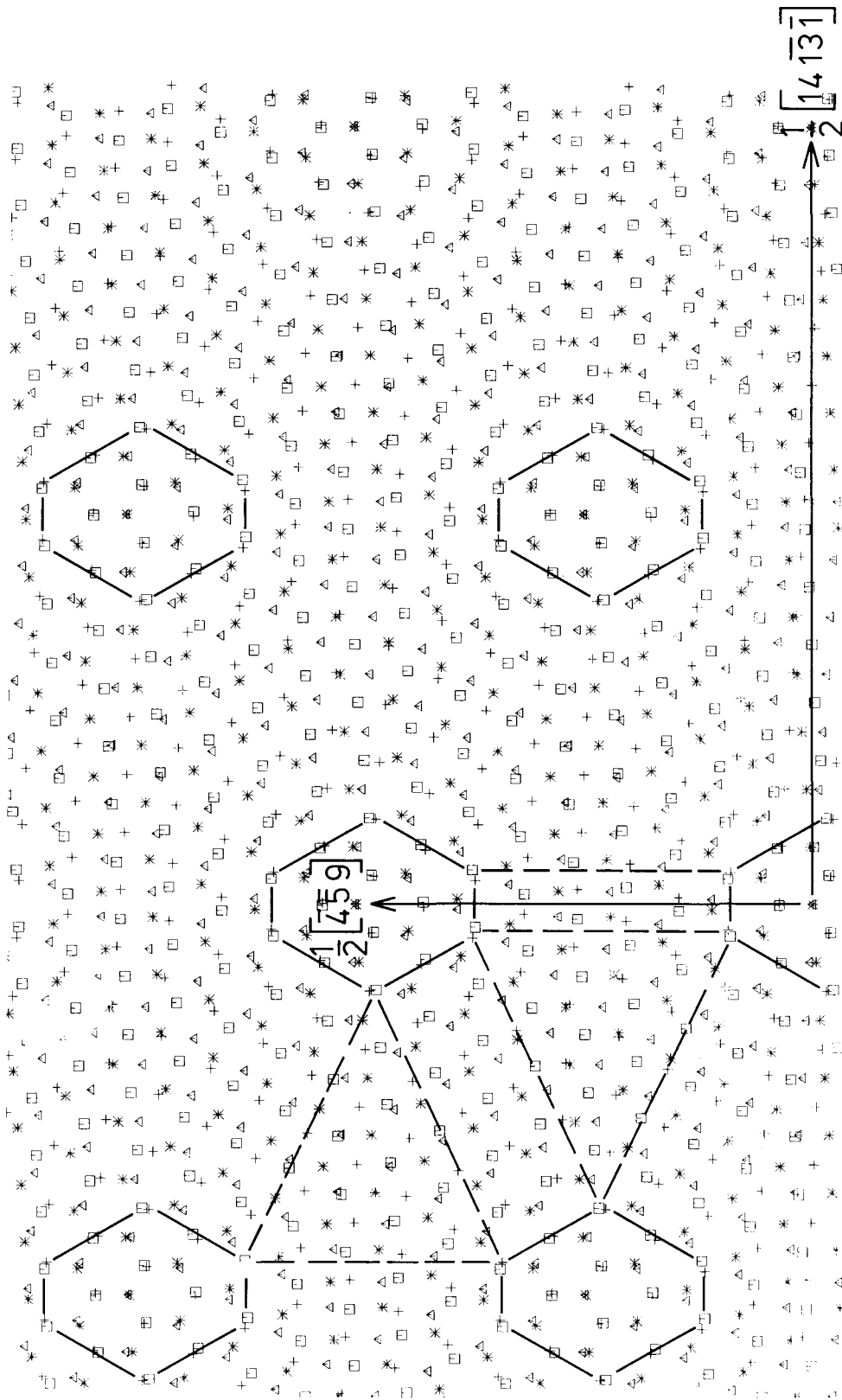
Structure of the $\Sigma = 61$ boundary: solid lines indicate distorted $\Sigma = 7$ units. Triangular regions (dashed line) of the $\Sigma = 3$ twin are surrounded by the network of the $\frac{1}{6}\langle 211\rangle$ DSC dislocations intersecting at $\Sigma = 7$ units.

corresponding dislocation contents of the boundaries, is an example of a generic result deduced on the basis of atomistic studies of grain boundary structures. Hence it is likely to be applicable to various types of tilt and twist boundaries. The results obtained here, indeed, show that structures of all the boundaries with misorientations between 0° and 21·79° ($\Sigma = 21$) are composed of units of the ideal lattice and/or the $\frac{1}{6}\langle 112 \rangle$ stacking fault on (111) planes, and units of the $\Sigma = 21$ boundary. Similarly, structures of boundaries with misorientations between 21·79° and 27·8° ($\Sigma = 13$), 27·8° and 38·21° ($\Sigma = 7$) and 38·21° and 60° ($\Sigma = 3$) can all be regarded as decomposed into units of the corresponding delimiting boundaries. The delimiting boundaries cannot be decomposed into any other structures and are thus favoured boundaries as defined by Sutton and Vitek (1983). In terms of the dislocation description the minority units can always be identified with intersections of dislocations forming a network possessing a three-fold symmetry and surrounding regions composed of majority units.

The dislocations present in the (111) twist boundaries are in most cases the DSC dislocations with the shortest possible Burgers vectors related to the CSL of the favoured boundary, the units of which are in the majority. There are, however, two notable exceptions. First, there are the low-angle boundaries in which the dislocations are the partial dislocations with Burgers vectors of the form $\frac{1}{6}\langle 112 \rangle$. As first suggested by Amelinckx (1964), the low-angle (111) twist boundary could be regarded as a hexagonal network of $\frac{1}{2}\langle 110 \rangle$ dislocations. However, in a $\{111\}$ plane these dislocations can, of course, dissociate into Shockley partials and it has been proposed by Scott and Goodhew (1981) that it is more favourable for every other node of the $\frac{1}{2}\langle 110 \rangle$ dislocations to dissociate, thus forming a triangular network of $\frac{1}{6}\langle 112 \rangle$ partials. This is indeed what has been found in our calculations and observed in gold using TEM (Scott and Goodhew 1981). This is also consistent with the earlier TEM observations of Schober and Balluffi (1969). Nevertheless, it should be mentioned that the interpretation of the contrast from dislocation networks in low-angle boundaries is complicated by the superposition of strain contrast from the network and interference (moiré) effects associated with the misorientation at the boundary. It has been shown (Hamelink and Schapink 1981, De Hosson *et al.* 1986) that, depending on the exact diffraction condition, the superposition may give rise to a hexagonal as well as a triangular type of contrast. This implies that the observation of a triangular network contrast cannot necessarily be interpreted in terms of the dissociation of a hexagonal network of screw dislocations as suggested by Scott and Goodhew (1981).

The second exception is the $\Sigma = 43$ boundary in which the grain boundary dislocations with the Burgers vectors $(1/14)\langle 541 \rangle$ and $(1/14)\langle 321 \rangle$ are present, rather than the DSC dislocations with the shortest possible Burgers vector related to $\Sigma = 21$, $(1/42)\langle 541 \rangle$. The latter dislocations, while having a small Burgers vector, are associated with a large step of height $\frac{1}{3}\langle 111 \rangle$ and it is, apparently, energetically more favourable when no steps are present in the boundary, even though the corresponding grain boundary dislocations must have in this case larger Burgers vectors. However, this feature of the grain boundary structure is not general, indeed, the $(1/42)\langle 541 \rangle$ DSC dislocations have been found in the $\Sigma = 67$ boundary. Whether dislocations possessing a short Burgers vector but associated with a step, or stepless dislocations with a longer Burgers vector, are energetically more favourable depends on the core structure of these dislocations. The present calculations suggest that for misorientations close to that of $\Sigma = 21$, DSC dislocations without a step will be present for misorientations smaller than 21·79°, whilst dislocations associated with a step will be present for misorientations larger than 21·79°. Unfortunately, no electron microscope

observations of dislocations in (111) twist boundaries with misorientations close to that of $\Sigma = 21$ have been made.

Steps are similarly associated with $\frac{1}{6}\langle 112 \rangle$ DSC dislocations present in the boundaries with the misorientation close to that of $\Sigma = 3$, as seen, for example, in the case of the $\Sigma = 61$ boundary (fig. 11). A number of experimental TEM observations of {111} twist boundaries with misorientations close to that of the $\Sigma = 3$ twin have been reported (Erlings and Schapink 1977, 1978, Hamelink and Schapink 1981, Scott and Goodhew 1981, De Hosson et al. 1986) and the observed dislocation configurations generally agree with the present calculations. Experimentally a triangular network of secondary GBDs with dislocation spacings in the range of 10–80 nm was observed in artificially fabricated bicrystals of gold. In the recent study of the Burgers vectors of secondary GBDs in high-angle grain boundaries near $\Sigma = 9$, 27 and 81 in specimens prepared from a bulk polycrystalline Cu–6 at.% Si alloy (Forwood and Clarebrough 1985, 1986), several twin boundaries near $\Sigma = 3$ twin were observed to contain networks of secondary GBDs with spacings of 300 nm. In contrast to the aforementioned observations and to our calculations, the latter coarse networks are hexagonal and triangular cells were not observed. However, as pointed out by Forwood and Clarebrough (1986), the steps associated with the hexagonal network could involve a small departure from the (111) plane giving a tilt component to the boundary.

The calculated misorientation-dependence of the grain boundary energy is in full agreement with the dislocation picture deduced on the basis of the atomic structure. Following the Read–Schockley type model described in §2, cusps occur at misorientations corresponding to the reference structures, and, as seen from fig. 1, these can be identified with the favoured boundaries found from structural considerations. As discussed in a previous study of the (001) twist boundaries (Vitek 1988), the shape of the cusps depends strongly on the energy, E_c, and the core radius, r_0, of the grain boundary dislocations. These have been determined in detail for the (001) twist boundaries but not in the present case, since an accurate determination of these quantities would require detailed atomistic calculations of much longer period boundaries with large values of Σ, as was done for the (001) twist boundaries (Vitek 1988). The depth of the cusps depends principally on the energy of the reference structure, γ_0. A very deep cusp occurs, therefore, at the misorientation corresponding to $\Sigma = 3$, since the coherent twist boundary possesses much lower energy than the other favoured boundaries. Nevertheless, the cusps associated with other favoured boundaries are well defined. This is in contrast with the case of (001) twist boundaries where the cusp of the same type is observed only for $\Sigma = 5$, while for the other favoured boundaries ($\Sigma = 13$ and 17) the cusps are either very shallow or appear as inflections rather than as well defined minima on the energy against misorientation curve. Hence any experimental study depending on the presence of cusps, such as the rotating ball experiments of Sautter, Gleiter and Bäro (1977) or rotating particle experiments of Chan and Balluffi (1985), should reveal their presence for twist boundaries on (111) much more readily than for (001).

REFERENCES

ACKLAND, G. J., TICHY, G., VITEK, V., and FINNIS, M. W., 1987, *Phil. Mag.* A, **56**, 735.

AMELINCKX, S.: *The direct observation of dislocations, Solid State Physics*, Suppl., **6**, p. 3.

BALLUFFI, R. W., 1982, *Metall. Trans.* A, **13**, 2069.

BALLUFFI, R. W., RÜHLE, M., and SUTTON, A. P., 1987, *Mater. Sci. Engng*, **89**, 1.

BLERIS, G. L., DELAVIGNETTE, P., 1981, *Acta crystallogr.* A, **37**, 779.

CHAN, S. W., and BALLUFFI, R. W., 1985, *Acta metall.*, **33**, 1113.

DAGENS, L., RASOLT, M., and TAYLOR, R., 1975, *Phys. Rev.* B, **11**, 2726.

DAW, M. S., and BASKES, M. I., 1984, *Phys. Rev.* B, **29**, 6443.

DE HOSSON, J. TH. M., SCHAPINK, F. W., HERINGA, J. R., and HAMELINK, J. J. C., 1986, *Acta metall.*, **34**, 1051.

DE HOSSON, J. TH. M., and VITEK, V., 1987, *Chemistry and Physics of Fracture*, edited by R. M. Latanision and R. H. Jones (Dordrecht: Martinus Nijhoff), p. 363.

DONI, E. G., BLERIS, G. L., KARAKOSTAS, TH., ANTONOPOULOS, J. G., and DELAVIGNETTE, P., 1985, *Acta crystallogr.* A, **41**, 440.

DUESBERRY, M. S., JACUCCI, G., and TAYLOR, R., 1979, *J. Phys.* F, **9**, 413.

ERLINGS, J. G., and SCHAPINK, F. W., 1977, *Scripta metall.*, **11**, 427; 1978, *Phys. Stat. sol.* (a), **46**, 653.

FINNIS, M. W., SINCLAIR, J. E., 1984, *Phil. Mag.*, **50**, 45.

FORWOOD, C. T., and CLAREBROUGH, L. M., 1985, *Aust. J. Phys.*, **38**, 449; 1986, *Phil. Mag.* A, **53**, L31.

FRANK, F. C., 1950, *Symposium on the Plastic Deformation of Crystalline Solids*, (ONR Pittsburgh), p. 150.

HAMELINK, J. J. C., and SCHAPINK, F. W., 1981, *Phil. Mag.* A, **44**, 1229.

HIRTH, J. P., and LOTHE, J., 1982, *Theory of Dislocations*, (New York: Wiley).

ISHIDA, Y., (editor), 1986, *Grain Boundary Structure and Related Phenomena, Trans. Japan Inst. Metals*, **27**, No. 1.

KING, A. H., 1982, *Acta metall.*, **30**, 419.

PETTIFOR, D. G., and WARD, M. A., 1984, *Solid St. Commun.*, **49**, 291.

READ, W. T., and SHOCKLEY, W., 1950, *Phys. Rev.*, **78**, 275.

RÜHLE, M., BALLUFFI, R. W., FISCHMEISTER, H., and SASS, S. L., (editors), 1985, *International Conference on the Structure and Properties of Internal Interfaces, J. Phys., Paris*, **46**, C4.

SASS, S. L., and RAJ, R., (editors), 1988, *Interface Science and Engineering '87, J. Phys., Paris*, (to be published).

SAUTTER, M., GLEITER, H., and BÄRO, G., 1977, *Acta metall.*, **25**, 467.

SCHWARTZ, D., SUTTON, A. P., and VITEK, V., 1985, *Phil. Mag.* A., **51**, 499.

SCHWARTZ, D., BRISTOWE, P. D., and VITEK, V., 1988, *Acta metall.*, **36**, 675.

SCHOBER, T., and BALLUFFI, R. E., 1969, *Phil. Mag.*, **20**, 511.

SCOTT, R. F., and GOODHEW, P. J., 1981, *Phil. Mag.* A, **44**, 373.

SUTTON, A. P., 1982, *Phil. Mag.* A, **46**, 171; 1984, *Int. Metals Rev.*, **29**, 377; 1988, *Acta metall.*, **36**, 1291.

SUTTON, A. P., and VITEK, V., 1983, *Phil. Trans. R. Soc. London*, A, **309**, 1.

VITEK, V., 1987, *Scripta metall.*, **21**, 711.

VITEK, V., and DE HOSSON, J. TH. M., 1986, *Computer-Based Microscopic Description of the Structure and Properties of Materials*, edited by J. Broughton, W. Krakow and S. T. Pantelides, *Mater. Res. Soc. Symp.*, **63**, 137.

VITEK, V., SUTTON, A. P., SMITH, D. A., and POND, R. C., 1980, *Grain Boundary Structure and Kinetics*, edited by R. W. Balluffi, (Ohio: American Society for Metals), p. 115.

WANG, G.-J., VITEK, V., and SUTTON, A. P., 1984, *Acta metall.*, **32**, 1093.

WOLF, D., and LUTSKO, J. F., 1989, *Atomistic Modeling of Materials: Beyond Pair Potentials*, edited by D. J. Srolovitz and V. Vitek, (New York: Plenum).

YOO, M. H., BRIANT, B. L., and CLARK, W. A. T., (editors), 1988, *Interfacial Structure and Design, Mater. Res. Soc. Symp.*, (to be published).